The Ror1 receptor tyrosine kinase plays a critical role in regulating satellite cell proliferation during regeneration of injured muscle

Received for publication, March 10, 2017, and in revised form, August 7, 2017 Published, Papers in Press, August 8, 2017, DOI 10.1074/jbc.M117.785709

Koki Kamizaki[‡1], **Ryosuke Doi**[‡1], **Makoto Hayashi**[‡1], **Takeshi Saji**[‡], **Motoi Kanagawa**[§], **Tatsushi Toda**[§], **So-ichiro Fukada**[¶], **Hsin-Yi Henry Ho**[‖2], **Michael Eldon Greenberg**[‖], **Mitsuharu Endo**[‡], **and Yasuhiro Minami**[‡3]

From the [‡]*Division of Cell Physiology, Department of Physiology and Cell Biology, and* [§]*Division of Neurology/Molecular Brain Science, Graduate School of Medicine, Kobe University, Kobe 650-0017, Japan, the* [¶]*Laboratory of Molecular and Cellular Physiology, Graduate School of Pharmaceutical Sciences, Osaka University, Osaka 565-0871, Japan, and the* [‖]*Department of Neurobiology, Harvard Medical School, Boston, Massachusetts 02115*

Edited by Joel Gottesfeld

The Ror family receptor tyrosine kinases, Ror1 and Ror2, play important roles in regulating developmental morphogenesis and tissue- and organogenesis, but their roles in tissue regeneration in adult animals remain largely unknown. In this study, we examined the expression and function of Ror1 and Ror2 during skeletal muscle regeneration. Using an *in vivo* skeletal muscle injury model, we show that expression of Ror1 and Ror2 in skeletal muscles is induced transiently by the inflammatory cytokines, TNF-α and IL-1β, after injury and that inhibition of TNF-α and IL-1β by neutralizing antibodies suppresses expression of *Ror1* and *Ror2* in injured muscles. Importantly, expression of *Ror1*, but not *Ror2*, was induced primarily in Pax7-positive satellite cells (SCs) after muscle injury, and administration of neutralizing antibodies decreased the proportion of Pax7-positive proliferative SCs after muscle injury. We also found that stimulation of a mouse myogenic cell line, C2C12 cells, with TNF-α or IL-1β induced expression of Ror1 via NF-κB activation and that suppressed expression of Ror1 inhibited their proliferative responses in SCs. Intriguingly, SC-specific depletion of *Ror1* decreased the number of Pax7-positive SCs after muscle injury. Collectively, these findings indicate for the first time that Ror1 has a critical role in regulating SC proliferation during skeletal muscle regeneration. We conclude that Ror1 might be a suitable target in the development of diagnostic and therapeutic approaches to manage muscular disorders.

The Ror family of receptor tyrosine kinases, Ror1 and Ror2, act as receptors for Wnt5a to activate the β-catenin-independent non-canonical Wnt signaling, thereby regulating cellular polarity, migration, proliferation, and differentiation during developmental morphogenesis and tissue- and/or organogenesis (1–8). Interestingly, Wnt5a–Ror1 and/or Wnt5a–Ror2 signaling also play important roles in the regulation of neural progenitor cells (NPCs)[4] and primordial germ cells (PGCs) during developmental processes (9, 10). It has also been shown that Wnt5a–Ror1 and Wnt5a–Ror2 signaling is required for the proliferation and stemness of NPCs and that Wnt5a–Ror2 signaling is involved in efficient polarization and migration of PGCs to the embryonic gonads in response to the chemotactic stem cell factor (SCF or secreted KitL). However, it remains largely unknown about possible roles of Ror1 and Ror2 in the regulation of adult tissue stem cells, including the skeletal muscle-specific stem cells.

Accumulating evidence further demonstrates that Wnt5a–Ror signaling is critically involved in various pathological conditions, including regeneration and/or inflammatory responses after tissue damage as well as cancer progression (11–15). Wnt5a–Ror2 signaling has been shown to be activated and to play crucial roles in inflammation by analyzing unilateral ureteral obstruction-induced kidney fibrosis and dextran sodium sulfate-induced colitis (15, 16). It has also been reported that inflammatory cytokines, including IL-6, activate Wnt5a–Ror2 signaling in adipose tissue-derived mesenchymal stem cells (17). Interestingly, it has been shown that Wnt5a–Ror2 signaling is required for intestinal crypt regeneration after injury (18) and that Ror2 plays an important role in regulating proliferative properties of reactive astrocytes after brain injury presumably independent of Wnt5a (19). However, the roles of Ror1 and Ror2 in regenerative processes are still poorly understood.

The skeletal muscles are one of the well-characterized locomotive organs, where skeletal muscle-specific stem cells (designated as satellite cells (SCs)) have been thought to play important roles during muscle regeneration after injury (20). SCs, which reside between the plasma membrane of myofibers and the basement membrane, are activated upon injury of the skel-

This work was supported by Grants-in-aid for Young Scientists (B) 15K18968 and 17K15596 (to M. H.), for Scientific Research (B) 16H05152 (to Y. M.), for Scientific Research on Innovative Areas 23112007 (to Y. M.), and for Challenging Exploratory Research 26670157 (to Y. M.) from the Ministry of Education, Culture, Sports, Science and Technology, Japan. The authors declare that they have no conflicts of interest with the contents of this article.

This article contains supplemental Figs. S1–S4.

[1] These authors contributed equally to this work.

[2] Present address: Dept. of Cell Biology and Human Anatomy, School of Medicine, University of California Davis, Davis, CA 95616.

[3] To whom correspondence should be addressed. Tel.: 81-78-382-5561; Fax: 81-78-382-5579; E-mail: minami@kobe-u.ac.jp.

[4] The abbreviations used are: NPC, neural progenitor cell; PGC, primordial germ cell; SC, satellite cell; PCP, planar cell polarity; CTX, cardiotoxin; TA, tibialis anterior; UC, unsorted cell; cKO, conditional knockout; PDTC, pyrrolidine dithiocarbamate; CSA, cross-sectional area; qRT, quantitative RT; PFA, paraformaldehyde.

etal muscles by physical accidents, extensive exercise, and so forth. During muscle regeneration, activated SCs proliferate and differentiate, eventually leading to formation of newly established myofibers by myoblast fusion (21, 22). This process is regulated elaborately by various cytokines and by expression of key transcriptional regulators such as paired box 7 (Pax7) and myogenic regulatory factors, which control specification and differentiation of SCs. It has been reported that inflammatory cytokines such as TNF-α and IL-1β are important for myogenesis (23–25). However, the roles of inflammatory cytokines in skeletal muscle regeneration are still somewhat controversial, and both cell growth-promoting and -inhibiting effects of inflammatory cytokines on SCs and/or myogenic cells have been reported (26).

It has been shown that both canonical and non-canonical Wnt signaling plays important roles in the proliferation and differentiation of SCs during muscle regeneration (27–32). For example, Wnt7a has been shown to promote proliferation of SCs through the β-catenin-independent Wnt/planar cell polarity (PCP) and Akt/mammalian target of rapamycin pathways upon binding to its receptor, Frizzled7 (Fzd7), during skeletal muscle regeneration (28, 33). Although both Ror1 and Ror2 have been shown to play important roles in the β-catenin-independent Wnt signaling, it remains unclear about their roles in the regulation of SCs during muscle regeneration after injury.

Here, we found that expression of Ror1 and Ror2 was induced by the inflammatory cytokines, TNF-α and IL-1β, in the skeletal muscle after injury and that induced expression of Ror1 in SCs was associated with their proliferative properties. We also sought to understand how *Ror1* is induced by inflammatory cytokines and to clarify the role of Ror1 in regulating properties of SCs and of a myogenic cell line, C2C12 cells.

Results

Expression of Ror1 and Ror2 is induced in injured skeletal muscles by TNF-α and IL-1β

We first examined temporal expression patterns of *Ror1* and *Ror2* mRNAs after the cardiotoxin (CTX)-induced injury of tibialis anterior (TA) muscles. We found that expression of *Ror1* and *Ror2* mRNAs was induced rapidly and reached maximal levels at day 3 and declined by day 7 after CTX-induced injury of TA muscles (Fig. 1*A*). It has been reported that inflammatory cytokines such as TNF-α and IL-1β are induced after damage of the skeletal muscles during the early phase of their regeneration (34). Thus, we examined temporal expression patterns of inflammatory cytokine mRNAs, including *Tnf-α* and *Il-1β* mRNAs, in the CTX-induced TA muscle-damage model. Importantly, expression of both *Tnf-α* and *Il-1β* was induced and reached maximal levels at day 1 and declined gradually at days 3 and 7 after TA muscle injury (Fig. 1*A*). The finding that the induced expression of *Tnf-α* and *Il-1β* precedes that of *Ror1* and *Ror2* during muscle regeneration suggests that expression of *Ror1* and *Ror2* could be regulated by TNF-α and IL-1β. We also assessed expression levels of Ror1 and Ror2 proteins during muscle regeneration. Expression of Ror1 and Ror2 proteins was detectable at days 1 and 3, respectively, reached maximal levels at day 7, and declined at day 14 after muscle injury (Fig. 1*B*).

Next, we examined the role of TNF-α and IL-1β in regulating expression of *Ror1* and *Ror2* induced by CTX-induced muscle injury. For this purpose, the effect of both TNF-α and IL-1β during muscle regeneration was inhibited by an administration of their neutralizing antibodies into the TA muscles treated with either PBS or CTX. It was found that blockade of TNF-α and IL-1β by neutralizing antibodies against them inhibited the induction of *Ror1* and *Ror2* following muscle injury compared with isotype-matched control IgG administration (Fig. 1*C*). Administration of the neutralizing antibodies or control IgG into the skeletal muscles injected with PBS failed to affect *Ror1* expression (Fig. 1*C*). Because blockade of TNF-α and IL-1β suppressed the induction of *Ror1* and *Ror2* expression in the damaged muscles, it can be assumed that TNF-α and/or IL-1β might regulate induced expression of *Ror1* and *Ror2* after muscle injury.

Expression of Ror1 is induced primarily in Pax7-positive SCs after injury of the skeletal muscles

We then examined which cells express *Ror1* and *Ror2* during muscle regeneration. To this end, we first separated SCs, which can be identified as SM/C-2.6-positive and CD31-, CD45-, and Sca-1-negative cells (35, 36), and unsorted cells (UCs) from the intact skeletal muscles (supplemental Fig. S1*A*), and we measured expression levels of *Ror1* and *Ror2* transcripts in SCs and UCs. As expected, expression of *Pax7*, one of the representative SC markers (37), was detected exclusively in SM/C-2.6-positive and CD31-, CD45-, and Sca-1-negative sorted SCs but not in UCs (Fig. 2*A, right panel*), indicating that these sorted cells indeed represent characteristics of SCs. Interestingly, expression of *Ror1* was detected primarily in sorted SCs (Fig. 2*A, left panel*). In contrast, expression of *Ror2* was detected in sorted SCs and UCs at comparable levels (Fig. 2*A, middle panel*). Based on this finding, we focused on Ror1 hereafter to elucidate its expression and function in sorted SCs in more detail.

Thus, we examined the proportions of SCs and expression levels of *Ror1* in SCs from the CTX-treated skeletal muscles at the indicated time points. The proportion of sorted SCs as well as the expression level of *Ror1* increased at day 3 and declined at day 12 after injury (supplemental Fig. S1, *B* and *C*). Furthermore, we examined expression of *Ror1* and *Pax7* in the respective sorted SCs from the intact and damaged skeletal muscles at day 3 by a multicolor fluorescence *in situ* hybridization (FISH) analysis with probes for *Ror1* mRNA and *Pax7* mRNA. In this analysis, these mRNAs could be detected as small particles, and we evaluated the numbers of the respective particles in the individual cells. Apparent *Ror1* mRNA particles were detectable in almost all the sorted SCs (Fig. 2*B, left panels*) but were rarely detectable in UCs from the intact muscles (Fig. 2, *C* and *E, left panels*). Importantly, increased numbers of *Ror1* mRNA particles per cell were observed in sorted SCs from injured muscles at day 3 compared with those from the intact muscles (Fig. 2, *B, right panels,* and *D* and *F*), but *Ror1* mRNA particles were marginally detectable in UCs from injured muscles (Fig. 2, *C* and *E, right panels*). We defined cells with one or more *Ror1* mRNA or *Pax7* mRNA particles as *Ror1*-positive or *Pax7*-positive cells,

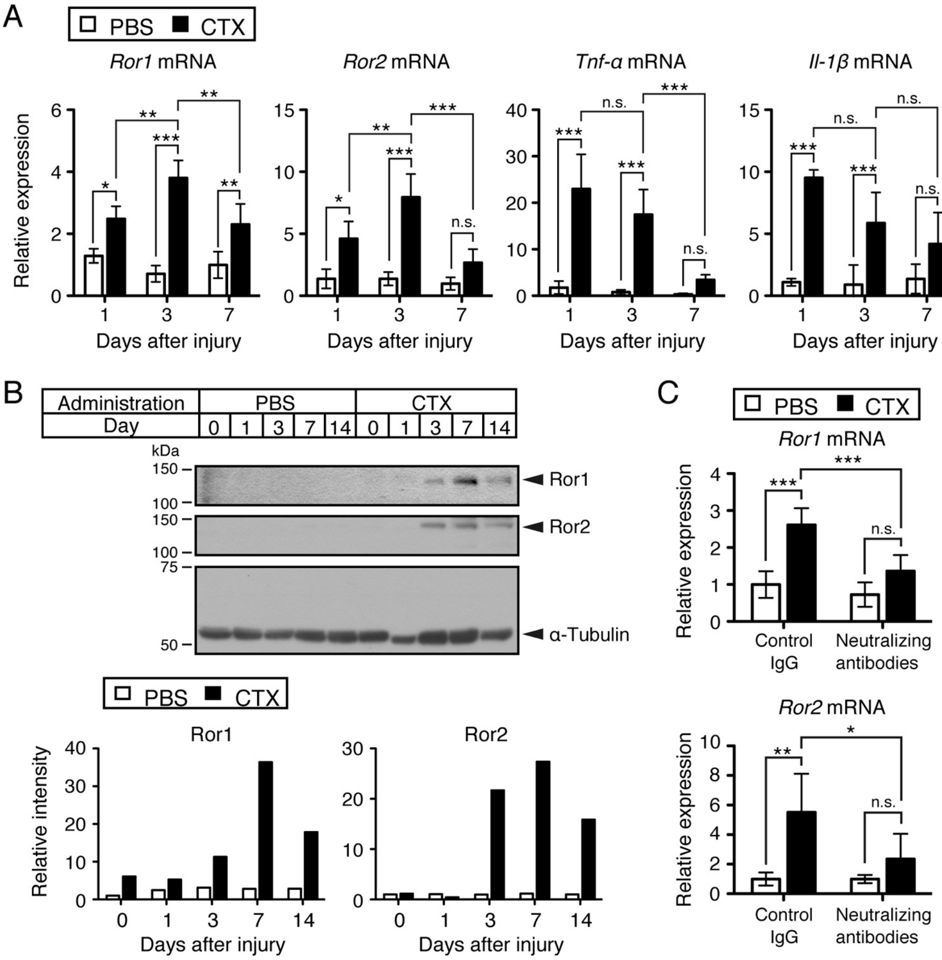

Figure 1. Induced expression of Ror1 and Ror2 following skeletal muscle damage by CTX can be inhibited by neutralizing antibodies against TNF-α and IL-1β. *A,* expression levels of *Ror1*, *Ror2*, *Tnf-α,* and *Il-1β* mRNAs in the skeletal muscles treated with either CTX or PBS were measured by qRT-PCR analysis at the indicated time points. Relative expression values were determined by defining expression levels (relative amounts) of the respective transcripts at day 0 (untreated) as 1. Data are expressed as mean ± S.D. ($n = 4$ animals). (*, $p < 0.05$; **, $p < 0.01$; ***, $p < 0.001$, *n.s.* (not significant), Bonferroni's post hoc test.) *B,* expression of Ror1 and Ror2 proteins is induced in the skeletal muscle following damage by CTX. Lysates were prepared from the skeletal muscles at the indicated time points after treatment with either CTX or PBS. Proteins (10 μg in total) in the respective lysates were separated by SDS-PAGE and separated proteins were subjected to Western blotting with anti-Ror1, anti-Ror2, and anti-α-tubulin antibodies, respectively. Based on these data, relative band intensities of Ror1 and Ror2 at the indicated time points were measured. Relative values were determined by defining expression levels of Ror1 or Ror2, respectively, at day 0 of PBS-treated skeletal muscles as 1. *C,* expression levels of *Ror1* mRNA and *Ror2* mRNA in the skeletal muscles treated with CTX or PBS in the presence of neutralizing antibodies against TNF-α and IL-1β or isotype-matched control IgG were measured by qRT-PCR analysis. Total mRNAs were prepared from the skeletal muscles 3 days after treatment with either CTX or PBS. Relative expression values of *Ror1* and *Ror2* were determined by defining expression level of *Ror1* or *Ror2*, respectively, at day 0 of PBS and control IgG-treated skeletal muscles as 1. Data are expressed as mean ± S.D. (PBS + control IgG, $n = 4$ animals; PBS + neutralizing antibodies, $n = 4$ animals; CTX + control IgG, $n = 6$ animals; CTX + neutralizing antibodies, $n = 6$ animals.) (*, $p < 0.05$; **, $p < 0.01$; ***, $p < 0.001$, *n.s.* (not significant), Bonferroni's post hoc test.)

respectively. The majority of *Pax7*-positive sorted SCs was also positive for *Ror1* (day 0 (intact), 86.44%, and day 3 (injured), 94.66%, Fig. 2*G*). These results indicate that *Ror1* is expressed in SCs and further induced in SCs after muscle injury.

Expression of Ror1 is induced via activation of NF-κB by TNF-α and IL-1β

We next performed experiments using from the mouse myogenic cell line C2C12 cells that have been utilized as an *in vitro* experimental model to study myogenic differentiation. In agreement with our findings using an injured skeletal muscle model, stimulation of C2C12 cells with either TNF-α or IL-1β resulted in induced expression of Ror1 at both mRNA and protein levels (Fig. 3, *A* and *B*), indicating that expression of *Ror1* could also be induced by TNF-α and IL-1β in the myogenic cells.

As an attempt to elucidate the molecular mechanism underlying induced expression of *Ror1* by TNF-α and/or IL-1β, we focused on the NF-κB signaling pathway, which can be activated in C2C12 cells by TNF-α and/or IL-1β (38). We examined the effect of the NF-κB inhibitor, pyrrolidine dithiocarbamate (PDTC), on TNF-α-induced expression of *Ror1*. Treatment of C2C12 cells with PDTC inhibited drastically TNF-α-induced expression of Ror1 at both mRNA and protein levels (Fig. 3, *C* and *D*). To further confirm NF-κB-mediated *Ror1* expression by TNF-α, we performed knockdown of p65, which is a component protein of the NF-κB complex, by treatment of C2C12 cells with two different siRNA oligonucleotides targeting *p65*. As shown, suppressed expression of p65 by siRNA inhibited significantly induced expression of Ror1 by TNF-α at both mRNA and protein levels (Fig. 3, *E* and *F*). Similar to TNF-α, induced expression of Ror1 by IL-1β was also

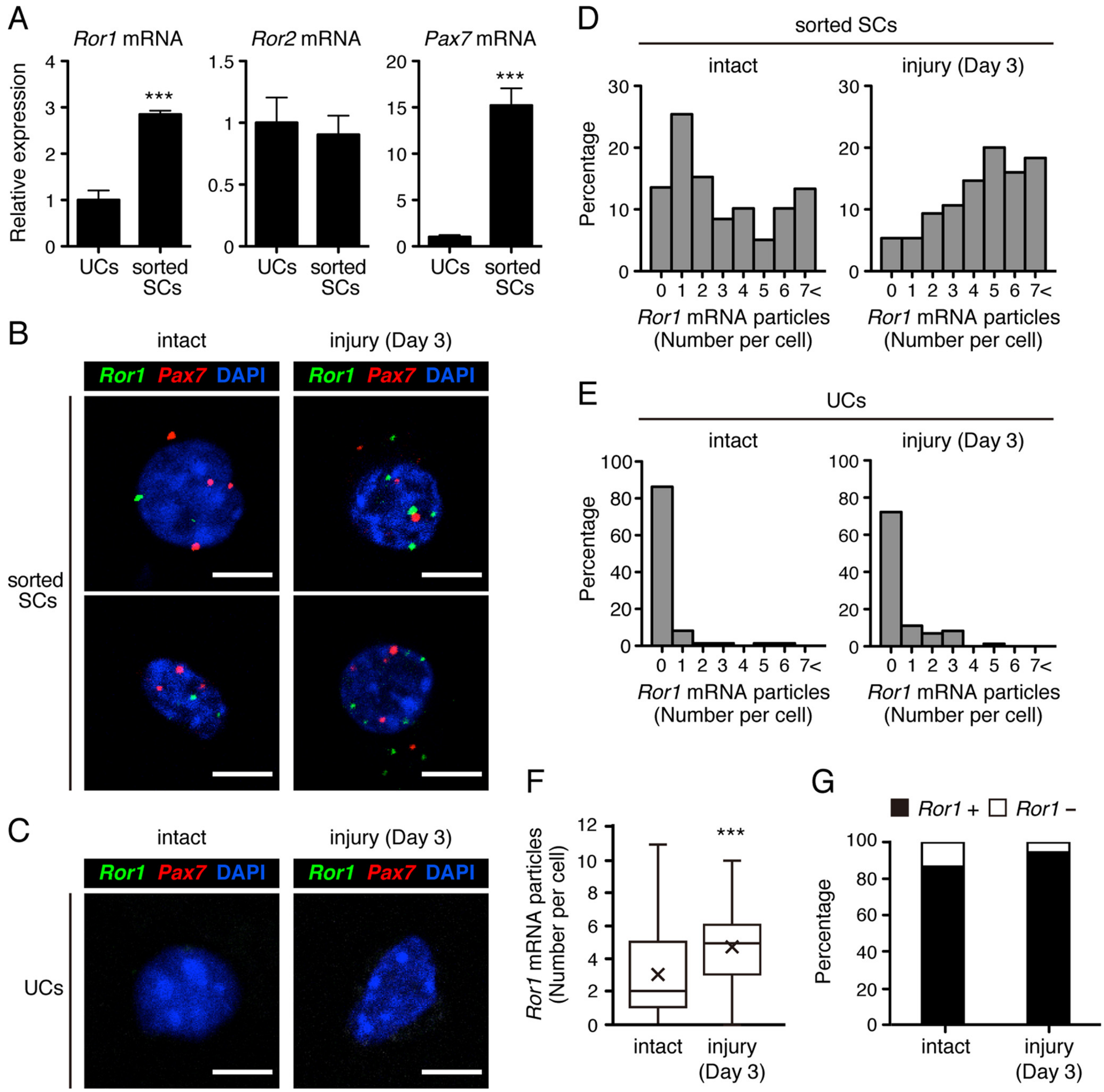

Figure 2. Expression of *Ror1* is induced primarily in Pax7-positive SCs following skeletal muscle damage by CTX. *A,* sorted SCs and UCs were separated from the intact skeletal muscles by FACS. Expression levels of *Ror1*, *Ror2*, and *Pax7* mRNAs in SCs and UCs were measured by qRT-PCR analysis. Relative expression values were determined by defining expression levels of the respective transcripts in UCs as 1. Data are expressed as mean ± S.D. ($n = 3$ animals). (***, $p < 0.001$, *t* test.) *B,* multicolor FISH analysis using probes for *Ror1* mRNA (*green*) and *Pax7* mRNA (*red*) in sorted SCs separated from the intact (*left panels*) or injured skeletal muscles (at day 3) (*right panels*). *Scale bar,* 5 μm. *C,* multicolor FISH analysis using probes for *Ror1* mRNA (*green*) and *Pax7* mRNA (*red*) in UCs separated from the intact (*left*) or injured skeletal muscles (at day 3) (*right panel*). *Scale bar,* 5 μm. *D–F,* quantification of the number of *Ror1* mRNA particles per *Pax7*-positive cell in sorted SCs separated from the intact (*D, left panels*) or injured skeletal muscles at day 3 after treatment with CTX (*D, right panels*) or in UCs from the intact (*E, left panels*) or injured skeletal muscles at day 3 after treatment with CTX (*E, right panels*). Data of sorted SCs are presented as histograms in *D* and *E* and box-and-whisker plots with average values (×) in *F* (intact (day 0); $n = 59$, injury (day 3); $n = 75$). (***, $p < 0.001$, *t* test.) *G,* percentage of *Ror1*-positive or -negative cells in *Pax7*-positive cells separated from the intact or injured skeletal muscles (at day 3).

abrogated by knockdown of *p65* (supplemental Fig. S2), indicating that induced expression of *Ror1* by TNF-α or IL-1β might be mediated by activation of the NF-κB pathway.

Because NF-κB has been shown to bind directly to a gene promoter and thereby activating transcription of target genes, we next investigated whether NF-κB might regulate transcriptional induction of *Ror1* directly by employing chromatin immunoprecipitation (ChIP) assay and luciferase reporter assay of the *Ror1* promoter. Sequence alignment of the human and mouse *Ror1* promoters revealed that two regions (region 1 and 2), containing putative NF-κB-binding sites (GGRRNNYYCC), are highly conserved between them (Fig. 4*A*) (39–41). Based on this sequence information, we designed three sets of primers to detect direct binding of p65 to three sites (sites 1–3, indicated in Fig. 4*A*) within the mouse *Ror1* promoter. ChIP assay revealed that stimulation of C2C12 cells with

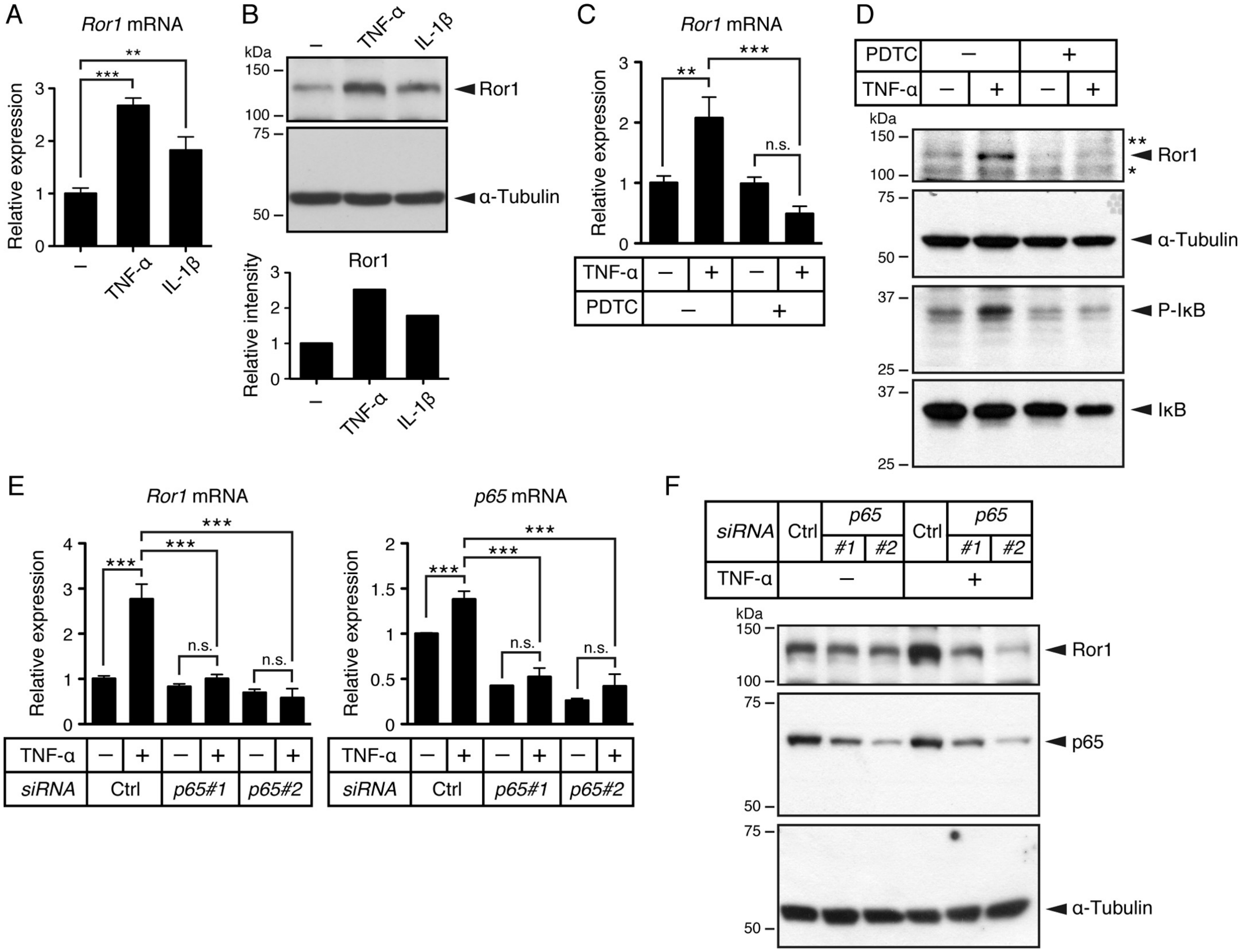

Figure 3. Expression of Ror1 induced by TNF-α is mediated by NF-κB pathway. *A,* expression level of *Ror1* mRNA in C2C12 cells treated with TNF-α (20 ng/ml), IL-1β (20 ng/ml), or vehicle alone (−) for 24 h was measured by qRT-PCR analysis. Relative expression values were determined by defining expression level of *Ror1* in cells treated with vehicle alone (−) as 1. Data are expressed as mean ± S.D. ($n = 3$). (**, $p < 0.01$; ***, $p < 0.001$, Bonferroni's post hoc test.) *B,* expression of Ror1 protein is induced in C2C12 cells treated with TNF-α (20 ng/ml) or IL-1β (20 ng/ml). Lysates (10 μg of proteins in total) prepared from C2C12 cells treated with TNF-α, IL-1β, or vehicle alone (−) for 24 h were subjected to SDS-PAGE and followed by Western blotting with anti-Ror1 or anti-α-tubulin antibodies, respectively. Relative band intensities of Ror1 were measured, and relative values were determined by defining expression level of Ror1 in vehicle alone (−) as 1. *C,* expression levels of *Ror1* mRNA in C2C12 cells treated with TNF-α (20 ng/ml) or vehicle alone (−) in the presence or absence of NF-κB inhibitor, PDTC (100 μM), for 24 h were measured by qRT-PCR analysis. Relative expression values were determined by defining expression level of *Ror1* in cells treated with vehicle alone as 1. Data are expressed as mean ± S.D. ($n = 3$). (**, $p < 0.01$; ***, $p < 0.001$, *n.s.* (not significant), Bonferroni's post hoc test.) *D,* relative band intensities of Ror1, phosphorylated IκB (*P-IκB*), IκB, and α-tubulin proteins in cell lysates (10 μg of proteins in total) from C2C12 cells treated with TNF-α (20 ng/ml) or vehicle alone (−) in the presence or absence of NF-κB inhibitor, PDTC (100 μM), for 24 h were measured by Western blotting with anti-Ror1, anti-phosphorylated IκB, anti-IκB, and anti-α-tubulin antibodies, respectively. Non-specific bands are indicated as * and **. *E,* expression of *Ror1* and *p65* mRNAs in C2C12 cells, transiently transfected with either *p65 siRNAs* (*p65#1* and *p65#2*) or control *siRNA* (*Ctrl*), followed by stimulation with TNF-α (20 ng/ml) or vehicle alone (−) for 24 h, was measured by qRT-PCR analysis. Relative expression values of *Ror1* and *p65* were determined by defining expression levels of *Ror1* or *p65*, respectively, in cells transfected with control *siRNA*, followed by treatment with vehicle alone as 1. Data are expressed as mean ± S.D. ($n = 3$). (***, $p < 0.001$, *n.s.* (not significant), Bonferroni's post hoc test.) *F,* Ror1, p65, and α-tubulin proteins in cell lysates (10 μg of proteins in total) from C2C12 cells transiently transfected with either *p65 siRNAs* or control *siRNA*, followed by stimulation with TNF-α or vehicle alone (−) for 24 h, were measured by Western blotting with anti-Ror1, anti-p65, or anti-α-tubulin antibodies, respectively.

TNF-α promoted the binding of p65 to sites 1–3 within the mouse *Ror1* promoter, similar to its binding to the *IκBα* promoter (a positive control for a p65 target gene), but it failed to promote its binding to a distal promoter region, about 20 kbps upstream of the *Ror1* promoter (a negative control for a p65 target gene) (Fig. 4*B*). We then examined whether the binding of p65 to the *Ror1* promoter might be required for transcriptional induction of *Ror1* by luciferase reporter assay. As shown in Fig. 4*C*, the DNA fragment from −1,000 to −500 base pairs (bps) (containing region 2), but not that from −500 to −1 bp, within the mouse *Ror1* promoter is required critically for responding to NF-κB activation induced by TNF-α. In fact, TNF-α-induced luciferase activities were suppressed by treatment with PDTC (Fig. 4*D*). Next, we examined whether putative p65-binding sites within region 2 are responsible for *Ror1* expression induced by stimulation with TNF-α. To this end, six putative p65-binding sites within the region 2 were deleted. Transfection with the p65-binding site-deleted reporter construct resulted in significant decreases in both basal and TNF-α-induced luciferase activities compared with transfection with

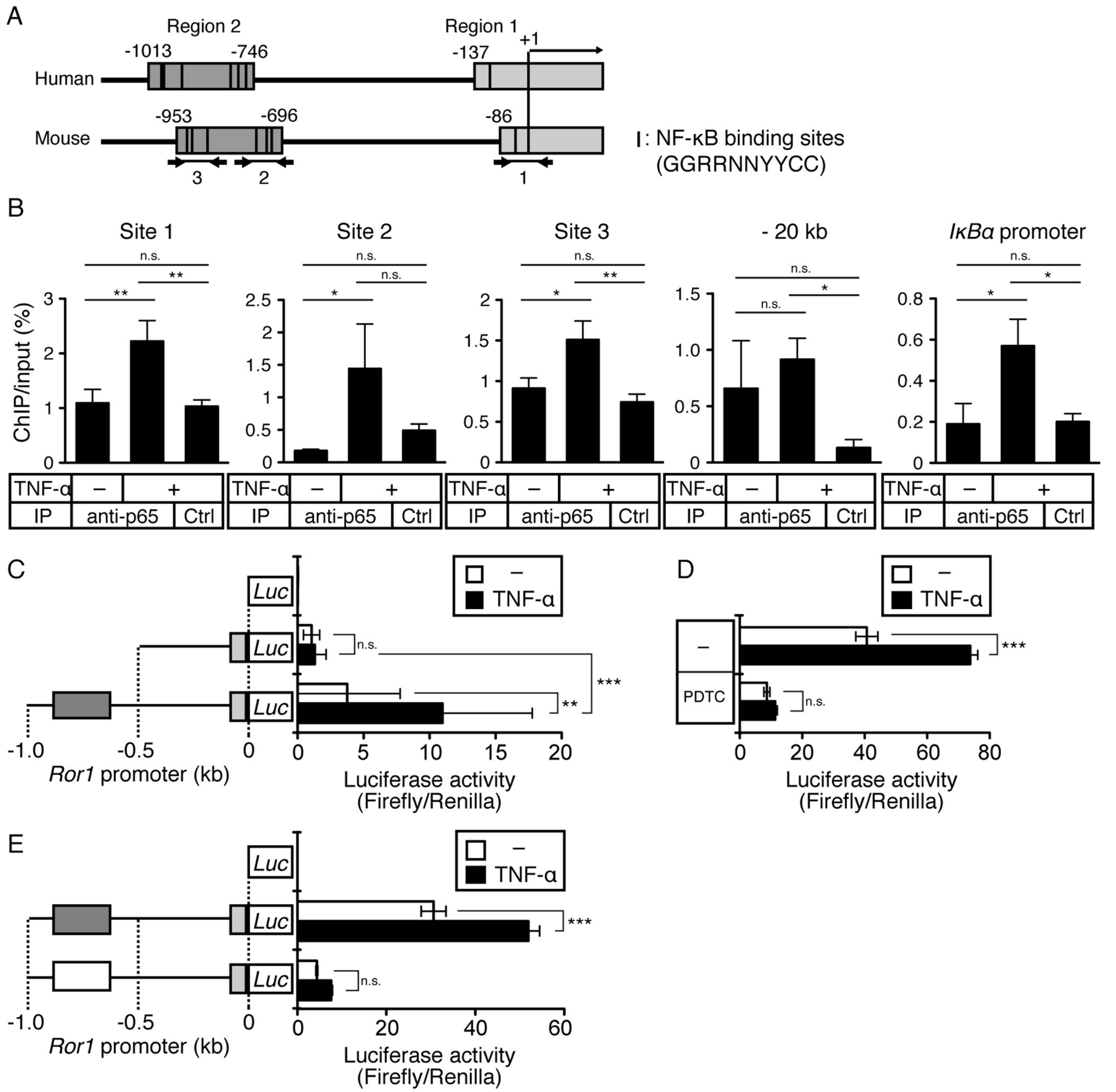

Figure 4. Expression of *Ror1* induced by TNF-α is mediated by direct binding of NF-κB to the promoter within *Ror1* gene. *A,* schematic representation of human and mouse *Ror1* promoters. Two regions (region 1 (*light gray boxes*) and region 2 (*dark gray boxes*)) are highly conserved between human and mouse *Ror1* genes. The *arrows* indicate the positions of primer sets for ChIP analysis. *Black lines* in regions 1 and 2 are putative NF-κB-binding sites (GG*RRNNYY*CC, *R* is A or G; N is any base; *Y* is C or T). *B,* binding of p65 to putative p65-binding sites within mouse *Ror1* promoter in C2C12 cells stimulated with TNF-α (20 ng/ml) was measured by ChIP analysis (see "Experimental procedures"). Lysates from C2C12 cells stimulated with TNF-α or vehicle alone (−) for 48 h were subjected to co-immunoprecipitation with either rabbit anti-p65 antibody or isotype-matched control (irrelevant) IgG (*Ctrl*), followed by qRT-PCR analysis using the above primer sets. The results of qRT-PCR with primer sets for the *IκBα* promoter and a distal *Ror1* promoter region (about 20 kbps upstream of the *Ror1* promoter) are shown as positive and negative control experiments, respectively. Representative data from three (*sites 1–3*) and two (*IκBα* promoter) independent experiments are shown. *Bars* represent the mean ± S.D. ($n = 3$). (*, $p < 0.05$; **, $p < 0.01$, Bonferroni's post hoc test). *IP,* immunoprecipitation. *C,* luciferase activities in C2C12 cells transiently transfected with control luciferase (*Luc*) reporter vector or *Luc* reporter vectors containing −0.5 or −1.0 kb mouse *Ror1* promoter, followed by stimulation with TNF-α (20 ng/ml) or vehicle alone (−) for 24 h, were measured as described under "Experimental procedures." Data are expressed as mean ± S.D. ($n = 6$). (**, $p < 0.01$; ***, $p < 0.001$, *n.s.* (not significant), Bonferroni's post hoc test.) *D,* luciferase activities in C2C12 cells transiently transfected with *Luc* reporter vectors containing −1.0-kbp mouse *Ror1* promoter, followed by stimulation with TNF-α (20 ng/ml) or vehicle alone (−) in presence or absence of NF-κB inhibitor, PDTC (20 μM), for 24 h were measured. Data are expressed as mean ± S.D. ($n = 3$). (***, $p < 0.001$, *n.s.* (not significant), Bonferroni's post hoc test.) *E,* luciferase activities in C2C12 cells transiently transfected with control *Luc* reporter, *Luc* reporter containing −1.0-kbp mouse *Ror1* promoter or *Luc* reporter containing −1.0-kbp mouse *Ror1* promoter with deletions of six putative p65-binding sites within region 2, followed by stimulation with TNF-α (20 ng/ml) or vehicle alone (−) for 24 h, were measured. Data are expressed as mean ± S.D. ($n = 3$). (***, $p < 0.001$, *n.s.* (not significant), Bonferroni's post hoc test.)

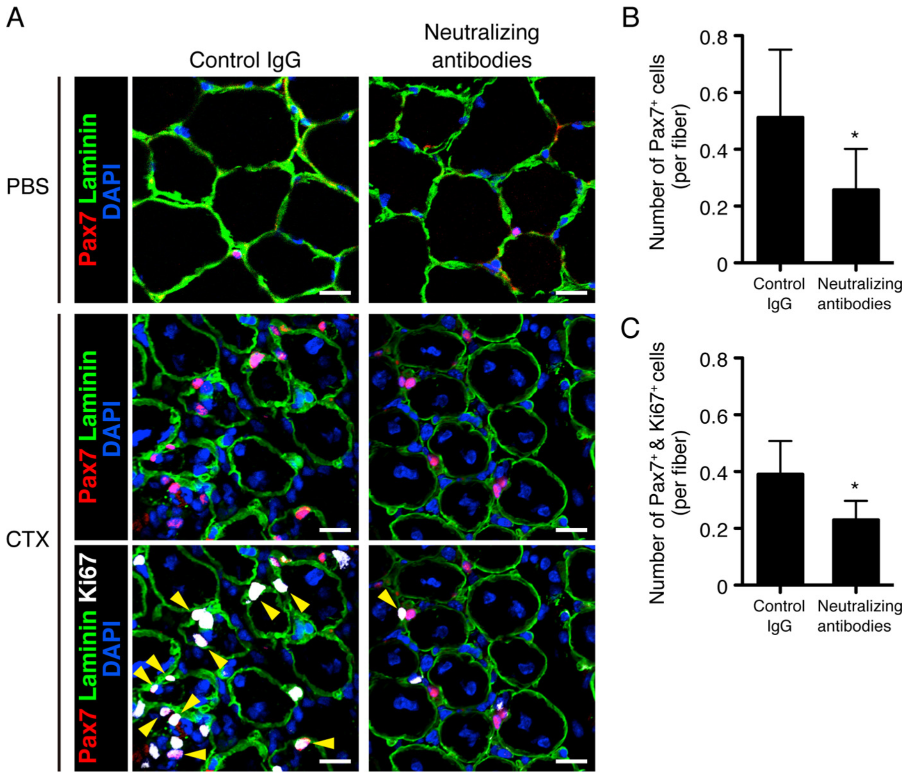

Figure 5. Proliferative SCs in the regenerating skeletal muscle are decreased by neutralizing antibodies against TNF-α and IL-1β. *A,* SCs (Pax7-positive cells, *upper* and *middle panels*) and proliferative SCs (Pax7 and Ki67-double positive cells, *lower panels, yellow arrowheads*) in the CTX-treated or -untreated skeletal muscles (at day 5) in the presence of neutralizing antibodies against TNF-α and IL-1β (*right panels*) or isotype-matched control IgG (*left panels*) were visualized by immunofluorescence staining with antibodies against Pax7 (*red*) and Ki67 (*white*). The numbers of SCs in CTX-untreated muscles in the presence of neutralizing antibodies or isotype-matched control IgG are 0.05 ± 0.015 or 0.07 ± 0.02 (not significant), respectively. Basement membranes and nuclei were visualized by staining with anti-laminin antibody (*green*) and DAPI (*blue*), respectively. *Scale bar,* 20 μm. *B,* number of Pax7-positive cells attached to a single myofiber in the CTX-treated skeletal muscles (at day 5) in the presence of neutralizing antibodies against TNF-α and IL-1β or isotype-matched control IgG were measured. Data are expressed as mean ± S.D. ($n = 8$ animals). (*, $p < 0.05$, *t* test.) *C,* number of Pax7 and Ki67-double positive cells attached to a single myofiber in the CTX-treated skeletal muscles (at day 5) in the presence of neutralizing antibodies against TNF-α and IL-1β or isotype-matched control IgG were measured. Data are expressed as mean ± S.D. ($n = 3$ animals). (*, $p < 0.05$, *t* test.)

the wild-type (control) reporter construct (Fig. 4*E*). The results indicate that induced expression of *Ror1* might be mediated directly by NF-κB activated by inflammatory cytokines, such as TNF-α and IL-1β.

Proliferative response of SCs is induced by TNF-α and IL-1β during muscle regeneration

Next, we examined the effect of TNF-α and IL-1β on the properties of SCs during muscle regeneration *in vivo* by ablation of TNF-α and IL-1β by their neutralizing antibodies. In the CTX-untreated muscles, any apparent differences in the number of SCs, characterized as Pax7-positive cells, were detected between control IgG-injected and neutralizing antibody-injected muscles (Fig. 5*A, upper panels*). However, ablation of both TNF-α and IL-1β in the damaged muscles reduced significantly the number of SCs compared with the muscles injected with control IgG (Fig. 5, *A, middle panels,* and *B*). Interestingly, co-immunostaining of Ki67 (a marker of proliferative cells) with Pax7 revealed that the number of proliferative SCs (Pax7- and Ki67-double positive cells) was also reduced by administration of neutralizing antibodies (Fig. 5, *A, lower panels,* and *C*), suggesting that TNF-α and IL-1β might regulate proliferative characteristics of SCs during muscle regeneration. Considering our findings that expression of Ror1 is induced in SCs by TNF-α and IL-1β during muscle regeneration, it is conceivable that Ror1 might play an important role in regulating proliferative property of SCs.

Ror1 is required for proliferative property of SCs during muscle regeneration

It has been reported that TNF-α stimulation induces proliferative response of C2C12 cells (24). To examine whether Ror1, induced by TNF-α, can affect property of myogenic C2C12 cells, we performed *Ror1* knockdown in C2C12 cells prior to their stimulation with TNF-α under differentiation conditions *in vitro*. As shown, TNF-α-induced *Ror1* expression was suppressed significantly by treatment with si-*Ror1#1* or *si-Ror1#2* (Fig. 6*A*). Consistent with the previous report, it was found that TNF-α stimulation induced some proliferative response of C2C12 cells as assessed by anti-Ki67 immunostaining (Fig. 6, *B* and *C*). Interestingly, suppressed expression of *Ror1* in C2C12 cells resulted in significant inhibition of TNF-α-induced proliferative response of C2C12 cells (Fig. 6, *B* and *C*), indicating that Ror1, induced by TNF-α, might be required for proliferative response of C2C12 cells.

To confirm the role of Ror1 in regulating proliferative response of SCs during muscle regeneration *in vivo*, we analyzed proliferation of SCs during the early phase of muscle regeneration using the mice lacking *Ror1* expression. Because conventional *Ror1* mutant mice die neonatally due to respira-

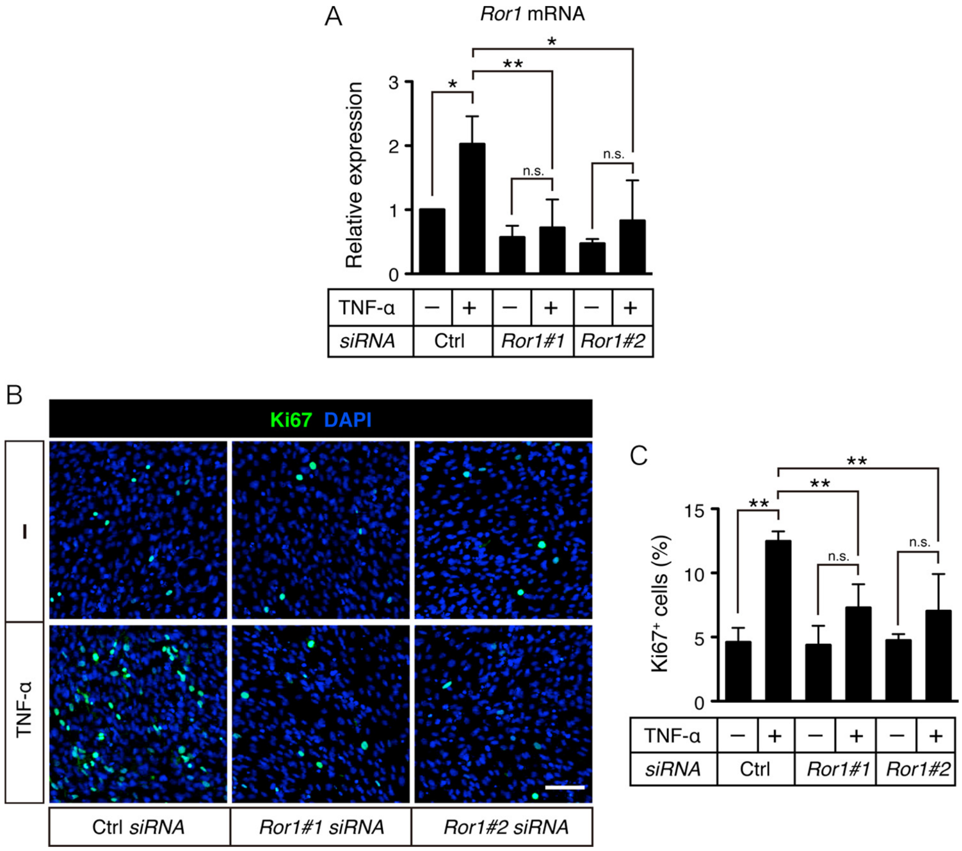

Figure 6. Ror1 is required for TNF-α-dependent proliferation of C2C12 cells. *A*, expression levels of *Ror1* mRNA in C2C12 cells, transiently transfected with either *Ror1 siRNAs* (*Ror1#1* and *Ror1#2*) or control *siRNA* (*Ctrl*), followed by stimulation with TNF-α (10 ng/ml) for 24 h, were measured by qRT-PCR analysis. Relative expression values were determined by defining expression level of *Ror1* in cells transfected with control *siRNA*, followed by treatment with vehicle alone as 1. Data are expressed as mean $\pm$ S.D. ($n = 3$). (*, $p < 0.05$; **, $p < 0.01$, *n.s.* (not significant), Bonferroni's post hoc test.) *B*, C2C12 cells, transiently transfected with either *Ror1 siRNAs* (*Ror1#1* and *Ror1#2*) or control *siRNA* (*Ctrl*), followed by stimulation with TNF-α (10 ng/ml) for 24 h, were visualized by staining with anti-Ki67 antibody (*green*) and DAPI (*blue*). *Scale bar*, 100 μm. *C*, proportions of Ki67-positive C2C12 cells were quantified. Data are expressed as mean $\pm$ S.D. ($n = 3$). (**, $p < 0.01$, *n.s.* (not significant), Bonferroni's post hoc test.)

tory dysfunction (42, 43), we established SC-specific *Ror1* conditional knock-out (*Ror1* cKO) mice. We separated SCs from the intact muscles of *Ror1* cKO mice after intraperitoneal injection of tamoxifen, and we measured the expression of *Pax7* and *Ror1* in sorted SCs and the other cells (UCs) to confirm SC-specific deletion of *Ror1*. qRT-PCR analysis revealed that expression of *Ror1* in the *Ror1* KO SCs was indeed almost undetectable compared with that in control SCs (Fig. 7*A*), whereas expression of *Pax7* in the *Ror1* KO SCs was almost unaffected (Fig. 7*A*). The result suggests that SC-specific *Ror1* deletion did not affect *Pax7* expression in SCs from the intact muscles. We then examined the effect of *Ror1* depletion in SCs on their proliferative property during muscle regeneration. To this end, we first analyzed expression of *Ror1* and *Pax7* in the damaged muscles from *Ror1* cKO and control mice at the indicated time points after CTX-induced muscle injury. As expected, basal and induced expression of *Ror1* in the damaged muscles from *Ror1* cKO mice was negligible during muscle regeneration, compared with those from control mice (Fig. 7*B, left panel*). Intriguingly, unlike the intact muscles, induced expression of *Pax7* was hardly detectable in the damaged muscles from *Ror1* cKO mice after injury, when compared with control mice (Fig. 7*B, right panel*). Importantly, immunofluorescent staining of SCs in the damaged muscle with anti-Pax7 antibody revealed that the number of Pax7-positive SCs per fiber in *Ror1* cKO mice reduced significantly compared with those in control mice (Fig. 7, *C* and *D*). FACS analysis further revealed that the proportion of SCs at the indicated time points after muscle injury increased at day 3 in control mice, but not *Ror1* cKO mice (Fig. 7*E* and supplemental Fig. S3). We also analyzed the cross-sectional area (CSA) of the TA muscles 14 days after CTX treatment. The median CSA of the TA muscles from *Ror1* cKO mice was significantly smaller than that from control mice (supplemental Fig. S4). Collectively, these findings indicate that Ror1 might play an important role in regulating proliferative property of SCs during muscle regeneration.

Discussion

Although the roles of Ror1 and Ror2 in adult animals have been extensively studied in the context of cancer progression and inflammation, little is known about their roles in tissue regeneration after injury. Thus far, it has been reported that Wnt5a–Ror2 signaling is required for intestinal crypt regeneration after microsurgical injury (18) and that Ror2 signaling plays an important role in regulating the proliferative response of reactive astrocytes after stub-wound injury of the brain cortex (19). However, it remains entirely unknown about the role of Ror1 in tissue regeneration after injury. In this study, we

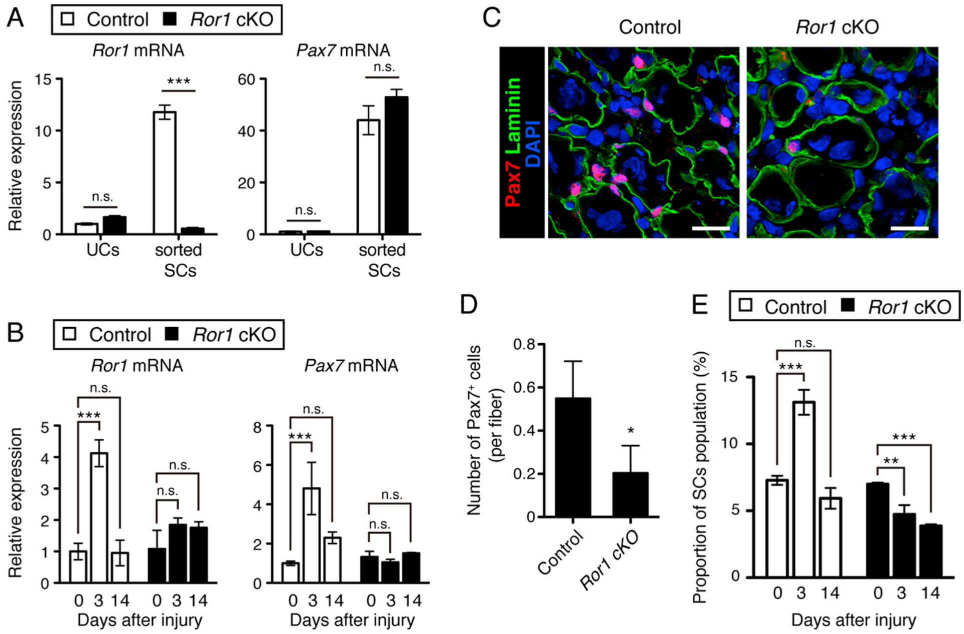

Figure 7. Ror1 deficiency in SCs suppresses injury-induced increase in their number. *A*, *Ror1*$^{flox/flox}$ (*Control*) and *Ror1*$^{flox/flox}$;*Pax7/Cre*$^{+/ERT2}$ (*Ror1* cKO) mice were injected intraperitoneally with tamoxifen once a day for 2 days, and then unsorted cells (*UCs*) and sorted SCs were isolated from the intact skeletal muscles by FACS (see "Experimental procedures"). Expression levels of *Ror1* and *Pax7* mRNAs in UCs and SCs were measured by qRT-PCR analysis. Data are expressed as mean ± S.D. ($n = 3$ animals). Relative expression values were determined by defining expression levels of the respective transcripts in UCs of control mice as 1. (***, $p < 0.001$, *n.s.* (not significant), Bonferroni's post hoc test.) *B*, expression levels of *Ror1* (*left panel*) and *Pax7* (*right panel*) mRNAs in the CTX-treated skeletal muscles at the indicated time points from control and *Ror1* cKO mice, injected intraperitoneally with tamoxifen once a day for 2 days prior to the treatment with CTX, were measured by qRT-PCR analysis. Relative expression values were determined by defining expression levels of the respective transcripts at day 0 of control mice as 1. Data are expressed as mean ± S.D. ($n = 3$ animals). (***, $p < 0.001$, *n.s.* (not significant), Bonferroni's post hoc test.) *C*, SCs (Pax7-positive cells) in the CTX-treated skeletal muscles (at day 5) from control (*left panel*) and *Ror1* cKO mice (*right panel*), injected intraperitoneally with tamoxifen once a day for 2 days prior to the treatment with CTX, were visualized by immunofluorescence staining with anti-Pax7 antibody (*red*). Basement membranes and nuclei were visualized by staining with anti-laminin antibody (*green*) and DAPI (*blue*), respectively. *Scale bar*, 20 μm. *D*, number of Pax7-positive cells attached to a single myofiber in the CTX-treated skeletal muscles (at day 5) from control and *Ror1* cKO mice, injected intraperitoneally with tamoxifen once a day for 2 days prior to the treatment with CTX, were measured. Data are expressed as mean ± S.D. ($n = 3$ animals). (*, $p < 0.05$, *t* test.) *E*, quantification of the SC proportion in the CTX-treated skeletal muscles at the indicated time points from control and *Ror1* cKO mice, injected intraperitoneally with tamoxifen once a day for 2 days prior to the treatment with CTX. Data are expressed as mean ± S.D. ($n = 3$ animals). (**, $p < 0.01$; ***, $p < 0.001$, *n.s.* (not significant), Bonferroni's post hoc test.)

show for the first time the critical role of Ror1 in regulating proliferative property of SCs during skeletal muscle regeneration. It was found that expression of *Ror1* could be detected mainly and constitutively in SCs and further induced in SCs after injury through NF-κB activation by TNF-α and IL-1β, and that induced expression of *Ror1* in SCs might play an important role in regulating their proliferative response.

It has been shown that Ror1 can act as a receptor for Wnt5a to mediate activation of NF-κB in leukemia B cells, HEK293 cells, and cochleae (44, 45). However, Wnt5a-independent functions of Ror1 in several cancer cells, including lung adenocarcinoma, have been reported (46, 47). Ror1 has been shown to associate with c-Met to mediate Met-driven cancer cell proliferation (46). Although our findings indicate the critical role of Ror1 in regulating proliferative property of SCs, the role of Wnt5a, whose expression is detectable during muscle regeneration *in vivo* (33), in this process remains unclear. We also observed expression of *Wnt5a* during muscle regeneration, but its temporal expression profile did not match the temporal proliferative response of SCs after muscle injury (data not shown). Expression of Wnt5a in C2C12 cells was also detectable at relatively lower levels, but it was affected marginally by stimulation with TNF-α and IL-1β (data not shown). At present, we also failed to detect Wnt5a-induced proliferative response of C2C12 cells in the presence or absence of TNF-α under our experimental setting (data not shown). Further study will be required to clarify a possible involvement of Wnt5a in Ror1-mediated regulation of SCs.

Supposing that the role of Ror1 in regulating the proliferative property of SCs during muscle regeneration might be independent of Wnt5a, it remains unclear about a responsible ligand for Ror1 to regulate the proliferative property of SCs during muscle regeneration. In this respect, it should be noted that *Wnt7a*, encoding another member of the Wnt family proteins, is induced during the early phase of muscle regeneration (33). Furthermore, Wnt7a and its cognate receptor Fzd7 play the critical role in regulating proliferation of SCs and myogenic cells through Wnt-PCP signaling during muscle regeneration (28, 33). Thus, it will be of interest to address a question of whether Ror1 is involved in Wnt7a–Fzd7 signaling by acting as a receptor or co-receptor for Wnt7a.

Our findings reveal that Ror1 might act as a novel molecule in SCs to regulate the proliferative property of SCs; however, it remains entirely unclear about the signaling pathway downstream of Ror1. Future studies will determine how Ror1 can regulate proliferative response of SCs during muscle regeneration. It can also be envisaged that Ror1 might be a suitable molecular target to develop novel diagnostic and therapeutic approaches to muscular disorders, including sarcopenia.

Experimental procedures

Mice

Male C57BL/6 mice at 8–12 weeks old were purchased from Japan SLC (Shizuoka, Japan). CTX (Latoxan, Valence, France)-induced TA muscle injury experiments were performed as described previously (48). Briefly, CTX (2.5 μl of 10 μM CTX/g body weight) or its vehicle alone (PBS) was injected into TA muscle unilaterally. In some experiments, neutralizing antibodies against TNF-α (0.5 μg/g body weight; eBioscience, Santa Clara, CA) and IL-1β (0.5 μg/g body weight; eBioscience) or isotype-matched control IgG (1.0 μg/g body weight; eBioscience) were co-injected with CTX or PBS. *Ror1*$^{flox/flox}$ mice were generated as described previously (49); *Pax7-Cre*$^{+/ERT2}$ mice were obtained from The Jackson Laboratory (50). For TA muscle injury, experiments of SC-specific *Ror1* knock-out mice, *Ror1*$^{flox/flox}$;*Pax7-Cre*$^{+/ERT2}$ mice were intraperitoneally injected with tamoxifen (100 μg/g body weight) (Sigma) once a day for 2 days, followed by injection with CTX into TA muscles. All animal experiments in this study were approved by the Institutional Animal Care and Use Committee (Permission No. P121005-R5) and conducted at the Institute for Experimental Animals, Kobe University Graduate School of Medicine, according to the Kobe University Animal Experimentation Regulations.

Isolation of SCs

TA muscles were digested in DMEM/F-12 containing 0.5% (w/v) collagenase type II (Worthington) for 90 min at 37 °C with trituration and passed through a 40-μm nylon mesh. The resultant cell suspensions were washed with ice-cold PBS containing 2% fetal bovine serum (FBS). SCs were isolated from the cell suspension by fluorescence-activated cell sorter (Moflo XDP, Beckman Coulter, Brea, CA) using anti-CD31, CD45, Sca-1, and SM/C-2.6 antibodies as described previously (35, 36, 48). SCs can be identified as SM/C-2.6-positive and CD31-, CD45-, and Sca-1-negative cells.

Fluorescence in situ hybridization (FISH)

To monitor the extent of *Ror1* expression in SCs, SCs isolated from intact or injured (at day 3) skeletal muscles by FACS were plated on a glass slide by Plate Spin2 (Kubota, Tokyo, Japan). SCs were then fixed with 4% (w/v) paraformaldehyde (PFA) for 10 min at room temperature and subjected to FISH analysis. FISH was carried out using a QuantGene ViewRNA *in situ* hybridization cell kit (Affymetrix, Santa Clara, CA) with the respective probe sets designed by Affymetrix for hybridization to mouse *Ror1* mRNA and *Pax7* mRNA, according to the manufacturer's instruction.

Immunofluorescence microscopic analysis

TA muscles were isolated, frozen with O.C.T. compound (Sakura Finetek, Tokyo, Japan), and sectioned in a cryostat. The frozen sections were fixed with 4% (w/v) PFA, permeabilized with 0.2% (v/v) Triton X-100/PBS, and blocked with M.O.M. Blocking Reagent (Vector Laboratories, Burlingame, CA). The sections were then stained with the respective antibodies and DAPI (Sigma). The following antibodies were used: anti-Pax7 (1:2, Developmental Studies Hybridoma Bank, Iowa City, IA), anti-Ki67 (14-5698-82, 1:100, eBioscience), and anti-laminin (L9393, 1:30, Sigma). Fluorescent images were obtained using a laser-scanning confocal imaging system (LSM710; Carl Zeiss, Oberkochen, Germany). Pax7-positive cells were defined as cells in which Pax7 was localized at the nuclei. To quantify the average of CSA, TA muscle sections stained with anti-laminin were analyzed by ImageJ.

Cell culture and transfection

Mouse myogenic cell line C2C12 cells were maintained in Dulbecco's modified Eagle's medium (DMEM; Nissui, Tokyo, Japan) supplemented with 20% FBS. C2C12 cells were stimulated with TNF-α (at a final concentration of 20 ng/ml; R&D Systems, Minneapolis, MN) or IL-1β (at a final concentration of 20 ng/ml; R&D Systems) in DMEM/F-12 supplemented with 2% horse serum. For blockade of NF-κB pathway, cells were pretreated with 100 μM pyrrolidine dithiocarbamate (PDTC, Merck Millipore, Darmstadt, Germany) for 1 h, followed by stimulation with TNF-α in the presence of 100 μM PDTC for 24 h. To inhibit expression of *p65* and *Ror1*, cells were transfected with the respective *siRNA* oligonucleotides by Lipofectamine RNAiMax reagent (Thermo Fisher Scientific, Waltham, MA). *siRNAs* targeting mouse *p65* (*p65#1*, Mm_Rela_0588; *p65#2*, Mm_Rela_0590) and their control *siRNA* (Mission siRNA universal negative control, catalog no. SIC_001) were purchased from Sigma. Silencer select *siRNAs* targeting mouse *Ror1* (*Ror1*#1, s77260; *Ror1*#2, s77261) and their control *siRNA* (Silencer select negative control no. 1, catalog no. 4390843) were purchased from Thermo Fisher Scientific. To examine proportions of Ki67-positive C2C12 cells, cells were transfected with the respective *siRNA* oligonucleotides and cultured in DMEM/F-12 supplemented with 2% horse serum in the presence or absence of TNF-α (at a final concentration of 10 ng/ml) for 24 h. The cells were fixed by 4% (w/v) PFA for 10 min at room temperature. The fixed cells were stained with the anti-Ki67 antibody along with DAPI to evaluate the percentages of Ki67-positive cells.

Real-time quantitative RT-PCR

Total RNAs were extracted from cultured cells and/or TA muscles using Isogen (Nippon Gene, Tokyo, Japan). cDNAs were synthesized from these RNAs as templates using PrimeScript RT reagent (Takara Bio, Shiga, Japan). Expression levels of the respective genes of interest were measured using the LightCycler 480 II system (Roche Applied Science, Basel, Switzerland). The amounts of mRNAs were normalized relative to those of *18S* ribosomal RNA. The sequences of the primer pairs are as follows: *Ror1* (5′-GCTGCGGATTAGAAACCTTG-3′ and 5′-TACGGCTGACAGAATCCATC-3′); *Ror2* (5′-ATGTGGACTCCCTCCAGATG-3′ and 5′-GAAGACGAAGTGGCAGAAGG-3′); *Tnf-α* (5′-ATGAGCACAGAAAGCATGATC-3′ and 5′-TACAGGCTTGTCACTCGAATT-3′); *Il-1β* (5′-CAGGATGAGGACATGAGCACC-3′ and 5′-CTCTGCAGACTCAAACTCCAC-3′); *Pax7* (5′-CTGGATGAGGGCTCAGATGT-3′ and 5′-GGTTAGCTCCTGCCTGCTTA-3′); and *p65* (5′-ATGGCTACTATGAGGCTGAC-3′ and 5′-GTCTCGCTTCTTCACACACT-3′).

Western blotting

Cells were solubilized in ice-cold lysis buffer (50 mM Tris-HCl (pH 7.5), 150 mM NaCl, 1% (v/v) Nonidet P-40, 1 mM EDTA, 10 mM NaF, 1 mM Na_3VO_4, 10 μg/ml aprotinin, 10 μg/ml leupeptin, 1 mM *p*-amidinophenylmethanesulfonyl fluoride). TA muscles were solubilized in ice-cold lysis buffer by using a homogenizer (Polytron homogenizer, Kinematica, Luzerne, Switzerland) for 30–60 s. Proteins (10 μg in total per lane) were separated by SDS-PAGE and transferred onto Immobilon-P membranes (Merck Millipore). Membranes were immunoblotted with the respective antibodies as follows: anti-Ror1 (catalog no. 4102, 1:5,000, Cell Signaling Technology, Danvers, MA); anti-α-tubulin (PM054-7, 1:5,000, Medical and Biological Laboratories, Nagoya, Japan); anti-p65 (catalog no. 8242, 1:5,000, Cell Signaling Technology); anti-phosphorylated IκB (catalog no. 2859, 1:1,000, Cell Signaling Technology), and anti-IκB (catalog no. 4814S, 1:1,000, Cell Signaling Technology). Immunoreactive bands were visualized by using Western Lightning Plus-ECL (PerkinElmer Life Sciences). Relative band intensities of the proteins of interest in Western blotting were quantified by ImageJ (National Institutes of Health, Bethesda, MD). Briefly, regions of interest were defined in the respective protein bands, and their intensities were measured by ImageJ.

Luciferase reporter assay

Mouse *Ror1* promoter regions from −500 to −1 bp or from −1,000 to −1 bp or from −1000 to −1 bp with deletion of six putative p65-binding sites within region 2 were subcloned into pGL4.10 (*Luc*) vectors (Promega, Madison, WI), respectively. Deletion construct was made by PrimeSTAR mutagenesis basal kit (Takara). These *Luc* vectors or an empty *Luc* vector were co-transfected with pRL-*TK* (Promega,) into C2C12 cells by Lipofectamine 3000 reagent (Thermo Fisher Scientific). Twenty hours after transfection, cells were further cultured in DMEM/F-12 supplemented with 2% horse serum in the presence or absence of TNF-α for 24 h. For blockade of NF-κB pathway, cells were pre-treated with 20 μM PDTC for 1 h, followed by stimulation with TNF-α in the presence of 20 μM PDTC for 24 h. Luciferase activities were measured using Dual-Luciferase reporter system (Promega) and GloMax 96 microplate luminometer (Promega). The transcriptional activities were normalized relative to *Renilla* luciferase activities.

ChIP assay

Samples were prepared using MAGnify chromatin immunoprecipitation system (Thermo Fisher Scientific). Briefly, cells were fixed with 1% (w/v) PFA for 10 min at room temperature and solubilized with cell lysis buffer (5 mM PIPES (pH 8.0), 8.5 mM KCl, 0.5% (v/v) Nonidet P-40, and protease inhibitors) for 10 min on ice. Subsequently, lysates were digested with 375 units/ml Micrococcal nuclease (Takara Bio) for 10 min at 37 °C. Nuclei were collected by centrifugation (500 × *g*) for 10 min at 4 °C and solubilized with Nuclei lysis buffer (50 mM Tris-HCl (pH 8.0), 10 mM EDTA (pH 8.0), and 1% SDS). Lysates were sonicated for three cycles (sonication, 30 s; on ice, 30 s) by a cell disruptor (UD-201, Tomy, Tokyo, Japan) and subjected to immunoprecipitation with anti-p65 (sc-372X, 1:20, Santa Cruz Biotechnology, Dallas, TX) or control rabbit IgG (011-000-003, 1:120, Jackson ImmunoResearch, West Grove, PA). After decross-linking and purification of the DNA fragments, the amounts of the DNA fragments of interest were measured by LightCycler 480 II system (Roche Applied Science) with the respective primer pairs and normalized relative to those in input materials. The sequences of the primer pairs are as follows: site 1 (5′-CCGAGATGCCTTGGAAGGTG-3′ and 5′-CTCCGACTGCAGAAGAGCG-3′); site 2 (5′-AAGTCAGTCTGGCATACAGTGG-3′ and 5′-TTACATACGGTGTATTTCTCTTGCT-3′); site 3 (5′-CACTGTCTATAATGCAGCAGGC-3′ and 5′-GAGTTCAGTACCAAGAACACCCT-3′); IκBα (5′-TAGCCAGCGTTTCCACTCTT-3′ and 5′-GGTCATGCACAGGGAACTTT-3′); about 20 kbps upstream of the *Ror1* promoter (5′-TGGAAAGCAATGATTTGACT-3′ and 5′-ATGCTTCCTAGGAGCTCTGT-3′).

Statistical analysis

Data are represented as the mean ± S.D. Statistical analyses were performed using the GraphPad Prism 5.0 (GraphPad Software). Statistical significance was determined as follows: *, $p < 0.05$; **, $p < 0.01$; ***, $p < 0.001$ and *n.s.* (not significant) compared with the corresponding control using the two-tailed Student's *t* test when two groups were compared and using one-way analysis of variance followed by Bonferroni's post hoc test when more than three groups were compared.

Author contributions—K. K., R. D., M. E., and Y. M. designed the research; K. K., R. D., M. H., and T. S. performed the experiments; M. K. and T. T. contributed to establish satellite cells and several mouse experiments; S. F. contributed to isolate SCs using SM/C-2.6 antibody and to perform several experiments with SCs; H. H. and M. E. G. contributed to establish Ror1 cKO mice and to perform experiments with them; K. K., R. D., M. H., M. E., and Y. M. wrote the manuscript.

Acknowledgments—We are grateful to S. Kato and Y. Okinaka (Kobe University) for helping to set up several experimental conditions and for technical assistance, respectively.

References

1. Minami, Y., Oishi, I., Endo, M., and Nishita, M. (2010) Ror-family receptor tyrosine kinases in noncanonical Wnt signaling: their implications in developmental morphogenesis and human diseases. *Dev. Dyn.* **239,** 1–15
2. Oishi, I., Suzuki, H., Onishi, N., Takada, R., Kani, S., Ohkawara, B., Koshida, I., Suzuki, K., Yamada, G., Schwabe, G. C., Mundlos, S., Shibuya, H., Takada, S., and Minami, Y. (2003) The receptor tyrosine kinase Ror2 is involved in non-canonical Wnt5a/JNK signalling pathway. *Genes Cells* **8,** 645–654
3. Schambony, A., and Wedlich, D. (2007) Wnt-5A/Ror2 regulate expression of XPAPC through an alternative noncanonical signaling pathway. *Dev. Cell* **12,** 779–792
4. He, F., Xiong, W., Yu, X., Espinoza-Lewis, R., Liu, C., Gu, S., Nishita, M., Suzuki, K., Yamada, G., Minami, Y., and Chen, Y. (2008) Wnt5a regulates directional cell migration and cell proliferation via Ror2-mediated noncanonical pathway in mammalian palate development. *Development* **135,** 3871–3879
5. Gao, B., Song, H., Bishop, K., Elliot, G., Garrett, L., English, M. A., Andre, P., Robinson, J., Sood, R., Minami, Y., Economides, A. N., and Yang, Y. (2011) Wnt signaling gradients establish planar cell polarity by inducing Vangl2 phosphorylation through Ror2. *Dev. Cell* **20,** 163–176
6. Nishita, M., Qiao, S., Miyamoto, M., Okinaka, Y., Yamada, M., Hashimoto, R., Iijima, K., Otani, H., Hartmann, C., Nishinakamura, R.,

and Minami, Y. (2014) Role of Wnt5a–Ror2 signaling in morphogenesis of the metanephric mesenchyme during ureteric budding. *Mol. Cell. Biol.* **34,** 3096–3105
7. Yamamoto, S., Nishimura, O., Misaki, K., Nishita, M., Minami, Y., Yonemura, S., Tarui, H., and Sasaki, H. (2008) Cthrc1 selectively activates the planar cell polarity pathway of Wnt signaling by stabilizing the Wnt-receptor complex. *Dev. Cell* **15,** 23–36
8. Green, J. L., Kuntz, S. G., and Sternberg, P. W. (2008) Ror receptor tyrosine kinases: orphans no more. *Trends Cell Biol.* **18,** 536–544
9. Endo, M., Doi, R., Nishita, M., and Minami, Y. (2012) Ror family receptor tyrosine kinases regulate the maintenance of neural progenitor cells in the developing neocortex. *J. Cell Sci.* **125,** 2017–2029
10. Laird, D. J., Altshuler-Keylin, S., Kissner, M. D., Zhou, X., and Anderson, K. V. (2011) Ror2 enhances polarity and directional migration of primordial germ cells. *PLoS Genet.* **7,** e1002428
11. Enomoto, M., Hayakawa, S., Itsukushima, S., Ren, D. Y., Matsuo, M., Tamada, K., Oneyama, C., Okada, M., Takumi, T., Nishita, M., and Minami, Y. (2009) Autonomous regulation of osteosarcoma cell invasiveness by Wnt5a/Ror2 signaling. *Oncogene* **28,** 3197–3208
12. Wright, T. M., Brannon, A. R., Gordan, J. D., Mikels, A. J., Mitchell, C., Chen, S., Espinosa, I., van de Rijn, M., Pruthi, R., Wallen, E., Edwards, L., Nusse, R., and Rathmell, W. K. (2009) Ror2, a developmentally regulated kinase, promotes tumor growth potential in renal cell carcinoma. *Oncogene* **28,** 2513–2523
13. Yamamoto, H., Oue, N., Sato, A., Hasegawa, Y., Yamamoto, H., Matsubara, A., Yasui, W., and Kikuchi, A. (2010) Wnt5a signaling is involved in the aggressiveness of prostate cancer and expression of metalloproteinase. *Oncogene* **29,** 2036–2046
14. Nishita, M., Enomoto, M., Yamagata, K., and Minami, Y. (2010) Cell/tissue-tropic functions of Wnt5a signaling in normal and cancer cells. *Trends Cell Biol.* **20,** 346–354
15. Sato, A., Kayama, H., Shojima, K., Matsumoto, S., Koyama, H., Minami, Y., Nojima, S., Morii, E., Honda, H., Takeda, K., and Kikuchi, A. (2015) The Wnt5a–Ror2 axis promotes the signaling circuit between interleukin-12 and interferon-γ in colitis. *Sci. Rep.* **5,** 10536
16. Li, X., Yamagata, K., Nishita, M., Endo, M., Arfian, N., Rikitake, Y., Emoto, N., Hirata, K., Tanaka, Y., and Minami, Y. (2013) Activation of Wnt5a–Ror2 signaling associated with epithelial-to-mesenchymal transition of tubular epithelial cells during renal fibrosis. *Genes Cells* **18,** 608–619
17. Fukuyo, S., Yamaoka, K., Sonomoto, K., Oshita, K., Okada, Y., Saito, K., Yoshida, Y., Kanazawa, T., Minami, Y., and Tanaka, Y. (2014) IL-6-accelerated calcification by induction of ROR2 in human adipose tissue-derived mesenchymal stem cells is STAT3-dependent. *Rheumatology* **53,** 1282–1290
18. Miyoshi, H., Ajima, R., Luo, C. T., Yamaguchi, T. P., and Stappenbeck, T. S. (2012) Wnt5a potentiates TGF-β signaling to promote colonic crypt regeneration after tissue injury. *Science* **338,** 108–113
19. Endo, M., Ubulkasim, G., Kobayashi, C., Onishi, R., Aiba, A., and Minami, Y. (2017) Critical role of Ror2 receptor tyrosine kinase in regulating cell cycle progression of reactive astrocytes following brain injury. *Glia* **65,** 182–197
20. Mauro, A. (1961) Satellite cell of skeletal muscle fibers. *J. Biophys. Biochem. Cytol.* **9,** 493–495
21. McGeachie, J. K., and Grounds, M. D. (1987) Initiation and duration of muscle precursor replication after mild and severe injury to skeletal muscle of mice. An autoradiographic study. *Cell Tissue Res.* **248,** 125–130
22. Chargé, S. B., and Rudnicki, M. A. (2004) Cellular and molecular regulation of muscle regeneration. *Physiol. Rev.* **84,** 209–238
23. Tidball, J. G. (2011) Mechanisms of muscle injury, repair, and regeneration. *Compr. Physiol* **1,** 2029–2062
24. Otis, J. S., Niccoli, S., Hawdon, N., Sarvas, J. L., Frye, M. A., Chicco, A. J., and Lees, S. J. (2014) Pro-inflammatory mediation of myoblast proliferation. *PLoS ONE* **9,** e92363
25. Chen, S. E., Jin, B., and Li, Y. P. (2007) TNF-α regulates myogenesis and muscle regeneration by activating p38 MAPK. *Am. J. Physiol. Cell Physiol.* **292,** C1660–C1671
26. Palacios, D., Mozzetta, C., Consalvi, S., Caretti, G., Saccone, V., Proserpio, V., Marquez, V. E., Valente, S., Mai, A., Forcales, S. V., Sartorelli, V., and Puri, P. L. (2010) TNF/p38α/polycomb signaling to Pax7 locus in satellite cells links inflammation to the epigenetic control of muscle regeneration. *Cell Stem Cell* **7,** 455–469
27. Otto, A., Schmidt, C., Luke, G., Allen, S., Valasek, P., Muntoni, F., Lawrence-Watt, D., and Patel, K. (2008) Canonical Wnt signalling induces satellite-cell proliferation during adult skeletal muscle regeneration. *J. Cell Sci.* **121,** 2939–2950
28. Le Grand, F., Jones, A. E., Seale, V., Scimè, A., and Rudnicki, M. A. (2009) Wnt7a activates the planar cell polarity pathway to drive the symmetric expansion of satellite stem cells. *Cell Stem Cell* **4,** 535–547
29. Tanaka, S., Terada, K., and Nohno, T. (2011) Canonical Wnt signaling is involved in switching from cell proliferation to myogenic differentiation of mouse myoblast cells. *J. Mol. Signal* **6,** 12
30. Bentzinger, C. F., von Maltzahn, J., Dumont, N. A., Stark, D. A., Wang, Y. X., Nhan, K., Frenette, J., Cornelison, D. D., and Rudnicki, M. A. (2014) Wnt7a stimulates myogenic stem cell motility and engraftment resulting in improved muscle strength. *J. Cell Biol.* **205,** 97–111
31. Parisi, A., Lacour, F., Giordani, L., Colnot, S., Maire, P., and Le Grand, F. (2015) APC is required for muscle stem cell proliferation and skeletal muscle tissue repair. *J. Cell Biol.* **210,** 717–726
32. von Maltzahn, J., Chang, N. C., Bentzinger, C. F., and Rudnicki, M. A. (2012) Wnt signaling in myogenesis. *Trends Cell Biol.* **22,** 602–609
33. von Maltzahn, J., Bentzinger, C. F., and Rudnicki, M. A. (2011) Wnt7a–Fzd7 signalling directly activates the Akt/mTOR anabolic growth pathway in skeletal muscle. *Nat. Cell Biol.* **14,** 186–191
34. Tidball, J. G. (2005) Inflammatory processes in muscle injury and repair. *Am. J. Physiol. Regul. Integr. Comp. Physiol.* **288,** R345–R353
35. Fukada, S., Higuchi, S., Segawa, M., Koda, K., Yamamoto, Y., Tsujikawa, K., Kohama, Y., Uezumi, A., Imamura, M., Miyagoe-Suzuki, Y., Takeda, S., and Yamamoto, H. (2004) Purification and cell-surface marker characterization of quiescent satellite cells from murine skeletal muscle by a novel monoclonal antibody. *Exp. Cell Res.* **296,** 245–255
36. Segawa, M., Fukada, S., Yamamoto, Y., Yahagi, H., Kanematsu, M., Sato, M., Ito, T., Uezumi, A., Hayashi, S., Miyagoe-Suzuki, Y., Takeda, S., Tsujikawa, K., and Yamamoto, H. (2008) Suppression of macrophage functions impairs skeletal muscle regeneration with severe fibrosis. *Exp. Cell Res.* **314,** 3232–3244
37. Seale, P., Sabourin, L. A., Girgis-Gabardo, A., Mansouri, A., Gruss, P., and Rudnicki, M. A. (2000) Pax7 is required for the specification of myogenic satellite cells. *Cell* **102,** 777–786
38. Langen, R. C., Schols, A. M., Kelders, M. C., Wouters, E. F., and Janssen-Heininger, Y. M. (2001) Inflammatory cytokines inhibit myogenic differentiation through activation of nuclear factor-κB. *FASEB J.* **15,** 1169–1180
39. Lenardo, M., Pierce, J. W., and Baltimore, D. (1987) Protein-binding sites in Ig gene enhancers determine transcriptional activity and inducibility. *Science* **236,** 1573–1577
40. de Martin, R., Vanhove, B., Cheng, Q., Hofer, E., Csizmadia, V., Winkler, H., and Bach, F. H. (1993) Cytokine-inducible expression in endothelial cells of an IκB α-like gene is regulated by NFκB. *EMBO J.* **12,** 2773–2779
41. Schindler, U., and Baichwal, V. R. (1994) Three NF-κB-binding sites in the human E-selectin gene required for maximal tumor necrosis factor α-induced expression. *Mol. Cell. Biol.* **14,** 5820–5831
42. Nomi, M., Oishi, I., Kani, S., Suzuki, H., Matsuda, T., Yoda, A., Kitamura, M., Itoh, K., Takeuchi, S., Takeda, K., Akira, S., Ikeya, M., Takada, S., and Minami, Y. (2001) Loss of mRor1 enhances the heart and skeletal abnormalities in mRor2-deficient mice: redundant and pleiotropic functions of mRor1 and mRor2 receptor tyrosine kinases. *Mol. Cell. Biol.* **21,** 8329–8335
43. Endo, M., Nishita, M., Doi, R., Hayashi, M., and Minami, Y. (2015) in *Receptor Tyrosine Kinases: Family and Subfamilies* (Wheeler, D. L., and Yarden, Y., eds) pp. 593–640, Springer International Publishing, Switzerland
44. Fukuda, T., Chen, L., Endo, T., Tang, L., Lu, D., Castro, J. E., Widhopf, G. F., 2nd, Rassenti, L. Z., Cantwell, M. J., Prussak, C. E., Carson, D. A., and Kipps, T. J. (2008) Antisera induced by infusions of autologous Ad-

CD154-leukemia B cells identify ROR1 as an oncofetal antigen and receptor for Wnt5a. *Proc. Natl. Acad. Sci. U.S.A.* **105,** 3047–3052
45. Diaz-Horta, O., Abad, C., Sennaroglu, L., Foster, J., 2nd, DeSmidt, A., Bademci, G., Tokgoz-Yilmaz, S., Duman, D., Cengiz, F. B., Grati, M., Fitoz, S., Liu, X. Z., Farooq, A., Imtiaz, F., Currall, B. B., *et al.* (2016) ROR1 is essential for proper innervation of auditory hair cells and hearing in humans and mice. *Proc. Natl. Acad. Sci. U.S.A.* **113,** 5993–5998
46. Gentile, A., Lazzari, L., Benvenuti, S., Trusolino, L., and Comoglio, P. M. (2011) Ror1 is a pseudokinase that is crucial for Met-driven tumorigenesis. *Cancer Res.* **71,** 3132–3141
47. Yamaguchi, T., Yanagisawa, K., Sugiyama, R., Hosono, Y., Shimada, Y., Arima, C., Kato, S., Tomida, S., Suzuki, M., Osada, H., and Takahashi, T. (2012) NKX2-1/TITF1/TTF-1-induced ROR1 is required to sustain EGFR survival signaling in lung adenocarcinoma. *Cancer Cell* **21,** 348–361
48. Doi, R., Endo, M., Yamakoshi, K., Yamanashi, Y., Nishita, M., Fukada, S., and Minami, Y. (2014) Critical role of Frizzled1 in age-related alterations of Wnt/β-catenin signal in myogenic cells during differentiation. *Genes Cells* **19,** 287–296
49. Ho, H. Y., Susman, M. W., Bikoff, J. B., Ryu, Y. K., Jonas, A. M., Hu, L., Kuruvilla, R., and Greenberg, M. E. (2012) Wnt5a–Ror-Dishevelled signaling constitutes a core developmental pathway that controls tissue morphogenesis. *Proc. Natl. Acad. Sci. U.S.A.* **109,** 4044–4051
50. Lepper, C., Conway, S. J., and Fan, C. M. (2009) Adult satellite cells and embryonic muscle progenitors have distinct genetic requirements. *Nature* **460,** 627–631